Experimental investigation on wake profile detection based on laser scattering by bubbles

Liping Su (苏丽萍), Weijiang Zhao (赵卫疆), Xiaoyong Hu (胡孝勇), Deming Ren (任德明), and Xizhan Liu (刘西站)

Institute of Opto-Electronics, Harbin Institute of Technology, Harbin 150080

Received April 16, 2007

The optical system for detecting wake profiles based on laser backscattering by bubbles at 180° is reported, in which the monostatic optical geometry is adopted and the power density estimation is used to process bubble scattering signal. The profiles of wakes produced by a two-blade propeller with a diameter of 46 mm at 6000 and 8000 rpm are measured using this system. It is shown that the wake region can be identified, the wake with different shapes can be distinguished, and the fine structure within wakes can be detected. Also, the repeatability of the results is tested experimentally. Results show the feasibility of this system in wake profile detection.

OCIS codes: 290.5820, 290.1350, 290.5850, 010.3640.

Recently, there is a great interest in studies on optical scattering properties of wake bubbles[1−5], which is the base of the technique for detecting and tracing fish stocks or ships by laser. Among the experimental investigations on optical scattering properties of bubbles in water, it is the most representative that Zhang *et al.* has measured the volume scattering function in a range of scattering angles of $10° - 170°$ for bubbles in natural water[1]. And other researches were mainly focused on the small-angle ($< 1.5°$) scattering in the forward direction[2]. Now a few authors have been preliminarily studying bubble backscattering at 180°[3,4]. However, those researches were limited on optical scattering properties of bubbles in water. In this paper, based on bubble backscattering at 180°, we report our work on the optical system for detecting wake profiles by laser from a wake-imaging point of view.

In this work, the detection object was the wake produced by using the self-developed two-blade propeller with a 46-mm diameter in the laboratory environment. The depth of water in the tank with size of $2(\mathrm{L}) \times 0.4(\mathrm{W}) \times 0.6(\mathrm{H})$ (m) was 41 cm. The center of the propeller was 20 cm to the bottom of the water tank. The driving system (as shown in Fig. 1) made the propeller rotate at the speed of 6000 or 8000 rpm. The wake produced by the propeller rotating at 6000 rpm was axisymmetric to spread out like a sector, but after about 10 s, the water tank was full of bubbles so that the wake profile was no longer clear. There was a very short cavity in the wake near the propeller axis, around which the bubble number rapidly increased, reaching to the maximum at a distance of the propeller radius to its axis, and then gradually decreased with the increase of the distance to the axis. However, the wake produced by the propeller at 8000 rpm was greatly different from that at 6000 rpm. Its profile was very clear to last for a period, longer than 10 s. It obviously became longer and was approximately a rectangular region where bubbles mainly located. But the cavitation disappeared.

The experimental setup is shown in Fig. 2. The optical system used a continuous wave (CW) single-longitudinal-mode frequency-doubled Nd:YAG laser as the light source, which emitted linearly polarized light with an output power of 20 mW and a beam divergence of 0.06°. The beam diameter was enlarged to 5 mm and the beam divergence reduced to 0.026° by a collimating and extender lens, which was composed of a 130-mm focal-length plano-concave lens and a 300-mm focal-length plano-convex lens. After expansion, the beam was separated into two beams by the beam splitter (BS) with transmissivity of 65%. The reflected beam entered into a reference detector, and the transmitted one passed through the 5-mm-diameter minipore at the center of the

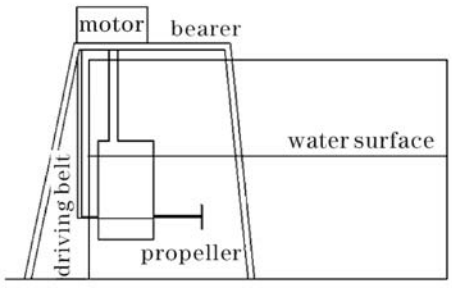

Fig. 1. Driving system of the propeller.

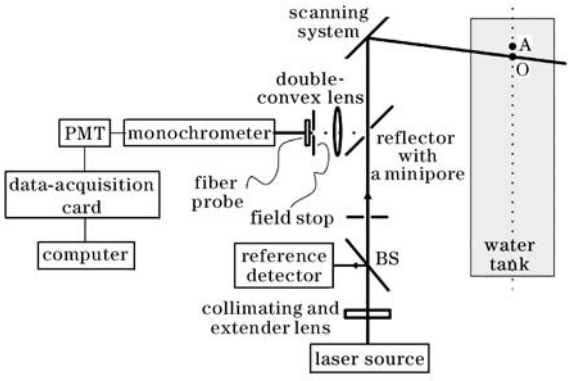

Fig. 2. Experimental setup for simulating the wake profile.

totally reflecting plane mirror with a 30-mm aperture, and then was redirected by the gold-plated reflecting mirror in the scanning equipment to illuminate bubbles in water. At the same time, this gold mirror redirected the scattering light from bubbles near 180° to the totally reflecting plane mirror that redirected it to a double-convex lens. It is obvious that the monostatic optical geometry can be realized by using the totally reflecting plane mirror and scanning system.

The scattering light was focused on the fiber probe with a masking aperture of 3 mm by the double-convex lens, coupled with the multimode fiber of 50-μm core diameter into a monochrometer (WDG500-1A), and then detected and converted into the electrical signals by the photomultiplier tube (PMT, GDB-27, Beijing Nuclear Instrument Factory). These electrical signals were captured with the data-acquisition card (PCI-6151, National Instruments) and finally delivered into the computer for data storage and processing. The field stop, with an aperture of 0.5 mm close to the fiber probe, reduced the response to extraneous light.

Besides the gold mirror, the scanning equipment included a horizontal turntable and a pitch motion, which supported the rotation within $0° - 360°$ with a 0.5° precision and tilting within $\pm 15°$ with a 0.5° precision, respectively, as shown in Fig. 3. Driven by the horizontal turntable, the gold mirror rotated in the horizontal plane (parallel to the paper plane), and driven by the pitch motion, it rotated in the vertical plane around the horizontal axis through its center.

The laser scanning area may be characterized by the region scanned by the beam on the back wall of the water tank. To repeat the experiment condition, we beforehand presented the specific scanning spots on the back wall of the water tank, as shown in Fig. 4. The x-y plane in the figure represents the vertical one where the back wall locates. The x axis, which is the projection of the propeller axial line on the x-y plane, represents the direction of the water tank length, and the y axis represents that of its height. The positive x axis is the water flow direction. Point A is the projection of the propeller center on the x-y plane. The origin O is the first scanning spot on the x axis. There are five horizontal and seven vertical scanning positions. In the two directions, the equal interval

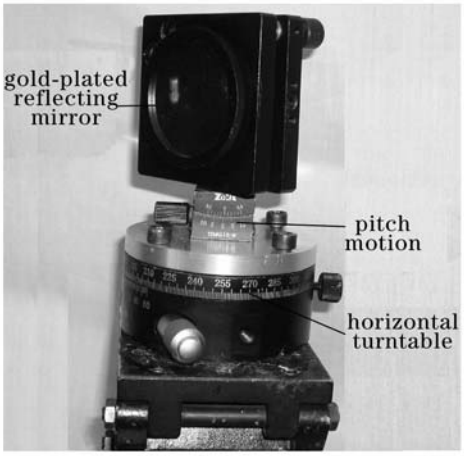

Fig. 3. Scanning equipment.

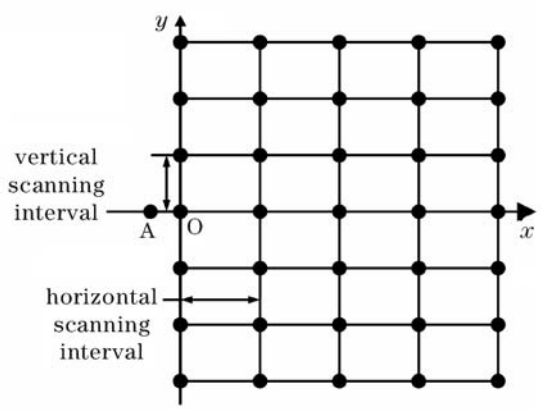

Fig. 4. Distribution of scanning spots.

scanning is carried out respectively and the scanning interval is determined according to practical situations.

The signal of bubble scattering is a series of discontinuous pulses and may be seen as a random quantity[6]. The sampling rate of the data-acquisition card is determined by the pulse width of bubble scattering signal. It was estimated that there was no pulse with a width of the magnitude of nanoseconds by using four kinds of the circuits that were composed of the oscillograph with the equivalent impedances of 1 MΩ and 50 Ω as well as the PMT with the load resistances of 67 kΩ and 50 Ω. So the sampling rate was selected to be 80 kHz and the load resistance of PMT was 67 kΩ, which determined the minimum pulse width of 25 μs.

Besides the bubble scattering pulse, there were the background light, the power frequency of 50 Hz and its harmonics as well as high-frequency noise in the measured signal. We used the power spectral density estimation to process the measured signal, which could make the various frequency components separate, eliminate those noises, and improve the signal-to-noise ratio (SNR). The average power of bubble scattering was the integral of the power spectral density over a certain frequency range of bubble scattering signal, and then 35 data were fit by spline interpolation to give the isoline map of the wake profile.

When the field stop was located respectively at, before and after the position of image of the propeller through the focusing lens, the wake profiles produced by the propeller at 6000 rpm were measured. Compared with the wake observed by eye, only when the field stop was at the position of the propeller image could the measured results not only portray the overall wake profile but also reflect the bubble distribution within the wake. This would relate to the depth of field of the receiving system. In fact, bubble backscattering near 180° measured using the monostatic optical geometry was not from a fixed scattering point or scattering volume, but from the optical pass within the receiving system's field of view (FOV), which would contain the non-wake region. Because the field stop was placed at position of the propeller image, the vertical plane through the propeller axis was located at the center of the depth of field. Therefore, the depth of field was mainly concentrated in the wake region and the scattering intensity from the wake region had a great proportion in the measured signal. Thus the

wake and non-wake region would be distinguished.

Using the 60- and 100-mm focal-length focusing lens, the wake profile at 6000 rpm was respectively measured when the field stop was at position of the propeller image. Compared with the observed wake by eye, the measured result using the 100-mm focal-length lens was more ideal. The depth of field decreased with the increase of the focal length of the lens. Therefore, the resolution of the optical system was enhanced when the focal length of the lens was 100 mm. In subsequent experiments, we used the 100-mm focal-length lens and placed the field stop at the position of the propeller image to eliminate influences of the receiving system on the simulation results of wakes.

Figure 5 shows the wake profiles produced by the propeller at 6000 rpm at the frequency ranges of bubble scattering signal of $500-1000$, $1000-2000$, $2000-3000$, and $3000-4000$ Hz. The horizontal scanning interval is 35 mm and the vertical one 25 mm. Each curve is the isoline of the normalized average power of bubble scattering given by the numerical values on this isoline. This normalized average power shows the magnitude of the scattering intensity, which can reflect the number of bubbles. The isoline density shows the variation of the scattering intensity in space, called the gradient which can reflect the variation of the bubble number in space. The position where the gradient dramatically changes is considered as the boundary between the wake and non-wake regions. The difference of the normalized average power between two adjacent isolines is 0.00365 in Fig. 5.

From Fig. 5(a), it can be seen that the scattering intensity gradually decreases and its gradient increases along the propeller axis at the vertical scanning distance of 0, whereas the scattering intensity and its gradient gradually decreases along the water flow direction at other vertical positions. It is also seen along the horizontal positive and negative axes that at the horizontal scanning distance less than 10 mm they increase first and decrease afterwards and reach to the maximum at the vertical positions of ± 23 and ± 37 mm respectively, while they both gradually decrease at the horizontal scanning distance greater than 10 mm.

The variation of the scattering intensity indicates that in the forward wake the bubble number is minimal around the propeller axis, then gradually increases first and decreases afterwards, resulting in the maximum at the vertical position of ± 23 mm, whereas the gradient variation indicates that the bubble number reduces fastest at the vertical position of ± 37 mm, thus these two positions are regarded as the boundary of the forward wake. It is obvious that the cavity, whose width is narrow and whose length is about 40 mm, appears in the wake profile at $500-1000$ Hz frequency range. However, the cavitation disappears in the wake profiles at other frequency ranges, as shown in Figs. 5(b)—(d). The frequency of the bubble scattering signal depends on the velocity and size of bubbles. The faster the bubbles move and the bigger they are, the lower the signal frequency is;

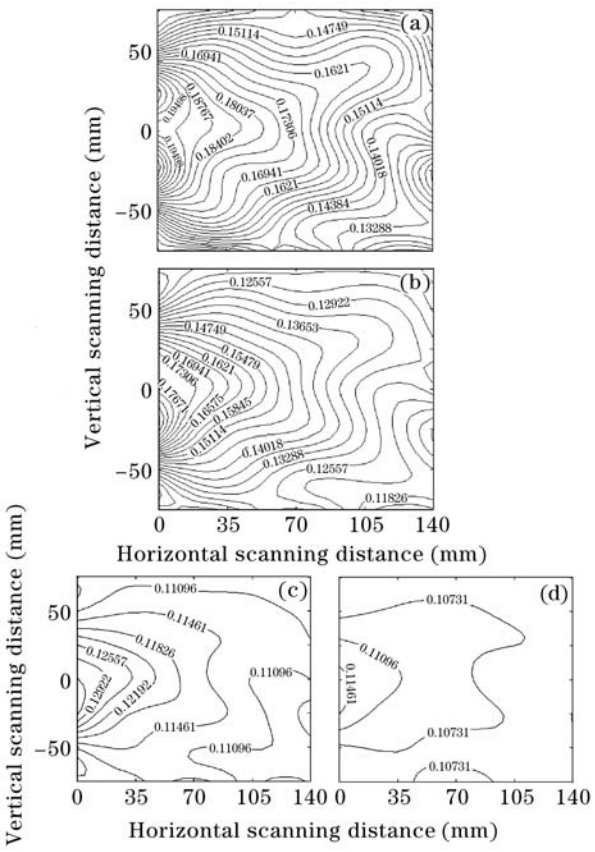

Fig. 5. Wake profiles produced by the propeller at 6000 rpm at the frequency ranges of (a) $500-1000$, (b) $1000-2000$, (c) $2000-3000$, (d) $3000-4000$ Hz.

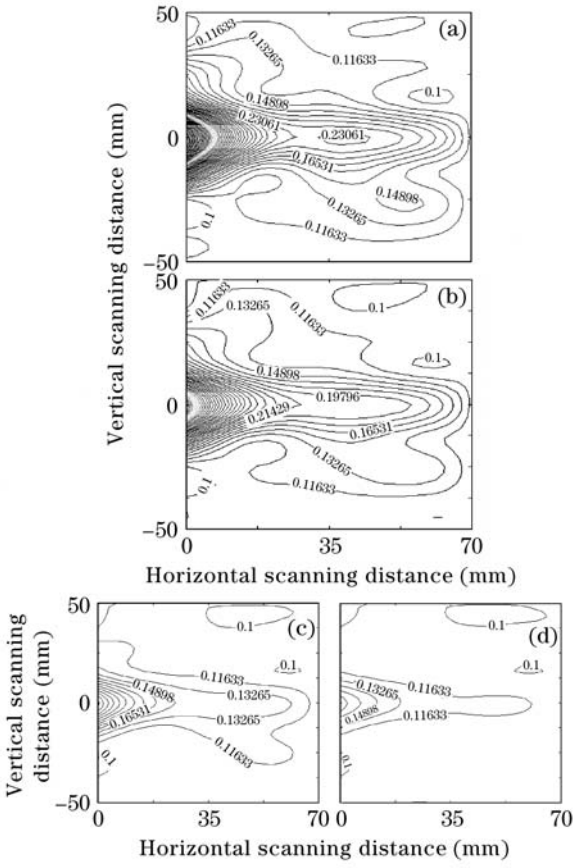

Fig. 6. Wake profiles produced by the propeller at 8000 rpm at the frequency ranges of (a) $500-1000$, (b) $1000-2000$, (c) $2000-3000$, (d) $3000-4000$ Hz.

otherwise it would be higher. Therefore, it is predicated that in the cavity there are relatively less low-velocity big bubbles, but lots of high-velocity small ones, which is difficult to be observed by eye.

In Fig. 5, the scattering intensity and its gradient at four frequency ranges are all approximately symmetric around the horizontal axis, which shows that the wake profile is axisymmetric with respect to the propeller axis. The results prove that the optical system may identify the wake region and detect the fine structure within the wake.

Figure 6 shows the wake profiles at 8000 rpm. The difference of the normalized average power between two adjacent isolines is 0.016. The gradient dramatically changes at the vertical position of ±22 mm, resulting in the wake-region width of 44 mm or so. The wake profile is approximately a rectangle region around the propeller axis. Moreover, the cavitation is not found in Fig. 6(a). These phenomena are in accordance with the observed results. From Fig. 6 we can conclude that the optical system can not only identify the wake region and detect the fine structure within the wake, but also distinguish wakes with different shapes.

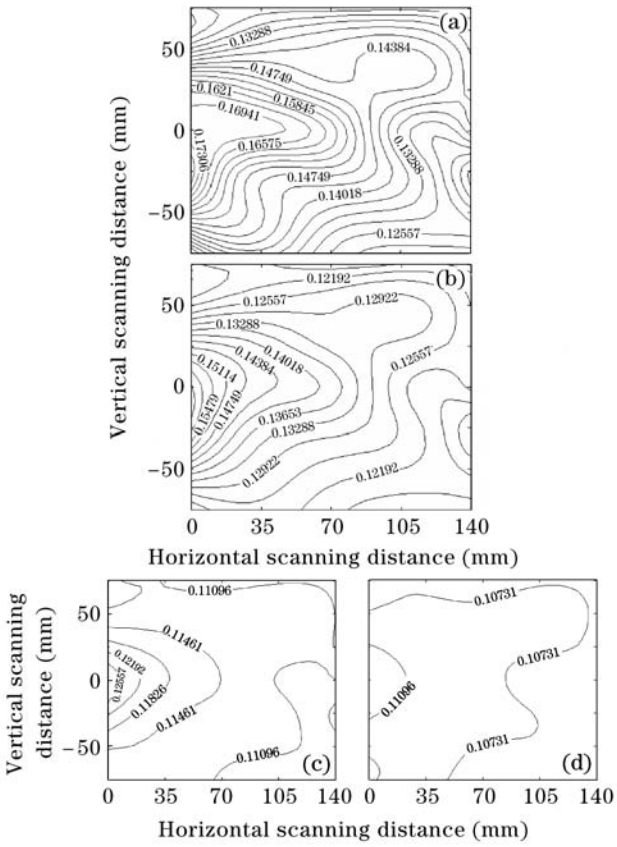

Fig. 7. Wake profiles produced by the propeller at 6000 rpm in repeated experiments at the frequency ranges of (a) 500 − 1000, (b) 1000 − 2000, (c) 2000 − 3000, (d) 3000 − 4000 Hz.

Many experiments were carried out on wakes of the propeller at 6000 and 8000 rpm under the same condition. Results show that the experiments are repeatable. Figure 7 shows the results of one of the experiments at 6000 rpm. The difference of the normalized average power between two adjacent isolines is 0.00365. Compared with Fig. 5, the scattering intensity slightly decreases, but other phenomena are similar. The cavity appears in the wake profile at 500 − 1000 Hz frequency range and the wake profiles at four frequency ranges are axisymmetric.

In conclusion, we have developed an optical system to detect wake profiles by laser based on bubble scattering at 180°. Influences of the position of field stop and the focal length of focusing lens on the measured profiles of wakes are analyzed. Using this system, the profiles of wakes of the propeller with a diameter of 46 mm at 6000 and 8000 rpm are successfully obtained, which shows that this system can identify the wake region, detect the fine structure within wakes, and distinguish wakes with different shapes. Our work provides an important guideline for the technique of detecting and tracing fish stocks or ships by laser.

This work was supported by the Program of Excellent Team in Harbin Institute of Technology. L. Su's e-mail address is laserslp@sohu.com.

References

1. X. Zhang and M. Lewis, Limnology and Oceanography **47,** 1273 (2002).
2. J. S. Zhang, J. K. Liu, Y. A. Zhang, B. J. Ji, and C. D. Sun, Journal of Xi'an Institute of Technology (in Chinese) **23,** 1 (2003).
3. J. A. Wang, X. Z. Jiang, Z. G. Ma, and S. G. Zong, Laser Technol. (in Chinese) **29,** 205 (2005).
4. Z. R. Li, J. F. Liu, and Z. F. Deng, Acta Photon. Sin. (in Chinese) **35,** 1417 (2006).
5. J. S. Zhang, J. H. He, B. J. Ji, and L. Y. Chen, Acta Photon. Sin. (in Chinese) **34,** 1275 (2005).
6. L. P. Su, W. J. Zhao, D. M. Ren, and X. Y. Hu, Proc. SPIE **6595,** 659524 (2007).